JOURNAL OF AGRICULTURAL AND FOOD CHEMISTRY

ARTICLE

pubs.acs.org/JAFC

# Evaluation of the Effect of Roasting on the Structure of Coffee Galactomannans Using Model Oligosaccharides

Ana S. P. Moreira,[†] Manuel A. Coimbra,[*,†] Fernando M. Nunes,[‡] Joana Simões,[†] and M. Rosário M. Domingues[†]

[†]QOPNA, Departamento de Química, Universidade de Aveiro, 3810-193 Aveiro, Portugal

[‡]Departamento de Química, Universidade de Trás-os-Montes e Alto Douro, 5001-801 Vila Real, Portugal

**ABSTRACT:** The roasting process induces structural changes in coffee galactomannans. To know more about the reaction pathways that occur during the roasting of coffee, mannosyl and galactomannosyl oligosaccharides, having a degree of polymerization (DP) between 3 and 4, were used as models for galactomannans. These compounds were dry-heated under air atmosphere from room temperature to 200 °C, being maintained at 200 °C for different periods of time. The roasted materials were analyzed by mass spectrometry (ESI-MS, MALDI-MS, and ESI-MS$^n$) and methylation analysis. In the MS spectra were identified several $[M + Na]^+$ ions belonging to a series from a single hexose to 10 hexose residues ($[Hex_{1-10} + Na]^+$). The ions corresponding to their respective mono- and tridehydrated derivatives ($[Hex_{2-10} - H_2O + Na]^+$ and $[Hex_{2-10} - 3H_2O + Na]^+$, respectively) were also identified. ESI-MS$^n$ as well as deuterium-labeling and alditol derivatization experiments showed that the tridehydrations occur at the reducing end of the oligosaccharides. The identification of (1→2)- and (1→6)-linked mannose residues and (1→4)-linked glucose residues by methylation analysis allowed the conclusion that transglycosylation and isomerization reactions occur during dry thermal processing.

**KEYWORDS:** dry thermal processing, coffee, manno-oligosaccharides, polysaccharides, mass spectrometry, electrospray ionization, MALDI

## INTRODUCTION

During the roasting process, the characteristic aroma, flavor, and color of roasted coffee beans are generated.[1,2] Roasting of coffee beans also improves the hot water extractability of their polysaccharides, namely, the galactomannans that become the major polysaccharide in roasted coffee infusions.[3−6] Apart from physical changes in the coffee beans that occur during the roasting process,[1,7] structural changes in coffee galactomannans have also been associated with the increase on their extractability in hot water.

Structurally, the galactomannans of green and roasted coffees have been described as linear polysaccharides with a main chain of β-(1→4)-linked D-mannose residues substituted at *O*-6 with side chains of single α-D-galactose residues.[3,8] However, some other structural features have also been reported, namely, the occurrence of β-(1→4)-linked D-glucose residues in the main backbone[9] and the presence of acetyl groups linked to mannose residues.[9−11] Also, side chains of single arabinose residues were found as structural features of green and roasted coffee galactomannans.[9] The roasting of coffee beans promotes the decrease of the degree of polymerization (DP) and debranching of the extractable galactomannans.[3,4,6,12] Furthermore, roasting promotes the occurrence of caramelization, isomerization, oxidation, decarboxylation, and Maillard reactions changing their reducing ends.[13] Despite the data already available, the chemical reactions that occur during the roasting of coffee, responsible for the change of the structural features of galactomannans, are not completely elucidated. This is mainly due to the complexity of the coffee bean[1] and heterogeneity of coffee galactomannans.[12] To know more about the products generated as a consequence of coffee roasting, in this study is proposed the use of model systems comprising a single population of molecules able to provide information concerning the specific reactions that can take place inside the coffee beans and can change the structure of their galactomannans. With this purpose, a thermal degradation mimicking the roasting conditions was induced independently in four oligosaccharides structurally related with coffee galactomannans.

Mass spectrometry, mainly tandem mass spectrometry (MS$^n$), using a soft ionization technique has been successfully used for the identification of detailed structural features of coffee galactomannans.[9,10,13] The analysis by MS allows information about monosaccharide composition and sequence, branching pattern, type of linkage, and presence of modifying chemical groups to be obtained, even when oligosaccharides are present in mixtures and with low abundance.[14,15] Thus, in the present work, thermally treated oligosaccharides were analyzed by MS using electrospray ionization (ESI) and matrix-assisted laser desorption/ionization (MALDI). MS data were complemented by information concerning the glycosidic linkage composition obtained by methylation analysis.

## MATERIALS AND METHODS

**Samples.** Oligosaccharide samples β-(1→4)-D-mannotriose ($Man_3$), [α-(1→6)-galactosyl][1]-β-(1→4)-D-mannobiose ($GalMan_2$), β-(1→4)-D-mannotetraose ($Man_4$), and [α-(1→6)-galactosyl][1]-β-(1→4)-D-mannotriose

Received: May 26, 2011
Revised: July 19, 2011
Accepted: August 6, 2011
Published: August 06, 2011

($GalMan_3$), having a white crystalline powder appearance and a purity of ≥95%, were obtained from Megazyme (County Wicklow, Ireland).

**Thermal Treatment of Samples.** The thermal treatments were performed with a thermogravimetric analyzer, model TGA-50 (Shimadzu, Kyoto, Japan), operating with a controlled air flow of 20 mL/min and a heating rate of 10 °C/min. All of the experiments were conducted using a platinum sample cell and an initial sample mass of 4−5 mg. Thermogravimetric (TG) curves as well as their first derivatives (DTG) were analyzed using Shimadzu TASYS software. To improve signal-to-noise ratios, the first derivatives of the original TG curves were smoothed using 100-point smoothing. The thermal stability of the $Man_3$ was studied by submitting it to a temperature program from ambient temperature to 600 °C. All of the samples under study were heated from room temperature to 200 °C (approximately 18 min), being maintained at 200 °C for different periods of time (0, 30, and 60 min). These different treatments are designated T1, T2, and T3, respectively, whereas the thermally untreated samples are designated T0. At the end of the treatments, the roasted materials were recuperated, weighed, and dissolved with Milli-Q high-purity water to give a concentration of about 5 mg/mL. To ensure the complete dissolution of these samples, they were stirred at 37 °C for 3 h and kept frozen at −20 °C until analysis. Solutions (approximately 1 mg/mL) of individual oligosaccharides without thermal treatment were prepared and stored according to the same procedure.

**Preparation of Oligosaccharide Alditols.** The $Man_3$ alditol derivatives were prepared according to the procedure described by Reis et al.[16] using sodium borohydride. Removal of sample contaminants is essential to successful mass spectrometry analysis.[17] To remove the excess of sodium ions, the final residue was dissolved in 1 mL of ultrapure water, and the solution was then exposed to Dowex 50W-X8 cation exchange resin (Bio-Rad Laboratories, Hercules, CA). Upon 30 min of incubation at room temperature, the solution was recovered, frozen, and freeze-dried.

**Preparation of Deuterium-Labeled Oligosaccharides.** To replace the hydrogen atom of hydroxyl groups by deuterium, 40 μL of the solutions of $Man_3$ and $GalMan_2$ subjected to the T2 thermal treatment was dried and then dissolved (40 μL) in deuterated water immediately before MS analysis.

**Electrospray Ionization Mass Spectrometry.** ESI-MS and ESI-$MS^n$ spectra of untreated and thermally treated oligosaccharides, as well as the deuterium-labeled ones, were carried out on an LXQ linear ion trap mass spectrometer (Thermo Fisher Scientific Inc., Waltham, MA). Typical operating conditions were as follows: electrospray voltage was 5 kV; capillary temperature was 275 °C; capillary voltage was 1 V; and tube lens voltage was 40 V. Samples were introduced at a flow rate of 8 μL/min into the ESI source. Nitrogen was used as nebulizing and drying gas. In the $MS^n$ experiments, the collision energy used was set between 18 and 31 (arbitrary units). Data acquisitions were carried out on an Xcalibur data system. ESI-MS and ESI-$MS^2$ spectra of $Man_3$ alditols were carried out on a Q-TOF2 hybrid tandem mass spectrometer (Micromass, Manchester, U.K.). The cone voltage was set at 35 V, and the capillary voltage was maintained at 3 kV. The source temperature was 80 °C, and the desolvation temperature was 150 °C. $MS^2$ spectra were obtained using argon as the collision gas, and the collision energy used was set between 25 and 30 eV. The raw data were processed using a MassLynx software (version 4.0). For all ESI analyses, samples dissolved in water were diluted in methanol/formic acid (99:1, v/v), and the spectra were acquired in the positive mode, scanning the mass range from $m/z$ 100 to 1500.

**Matrix-Assisted Laser Desorption/Ionization Spectrometry.** Sample preparation for MALDI analysis was performed by deposition of 0.5 μL of sample dissolved in water on top of a layer of crystals of 2,5-dihydroxybenzoic acid (DHB) formed by deposition of 0.5 μL of DHB solution on the MALDI plate and letting it dry at room temperature. The matrix solution was prepared by dissolving 5 mg of DHB in a 1 mL mixture of acetonitrile/methanol/aqueous trifluoroacetic acid (1%, v/v) (1:1:1, v/v/v). MALDI mass spectra were acquired using a MALDI-TOF/TOF Applied Biosystems 4800 Proteomics Analyzer (Applied Biosystems, Framingham, MA) instrument equipped with a nitrogen laser emitting at 337 nm and operating in a reflectron mode. Full-scan mass spectra ranging from $m/z$ 500 to 4000 were acquired in the positive mode.

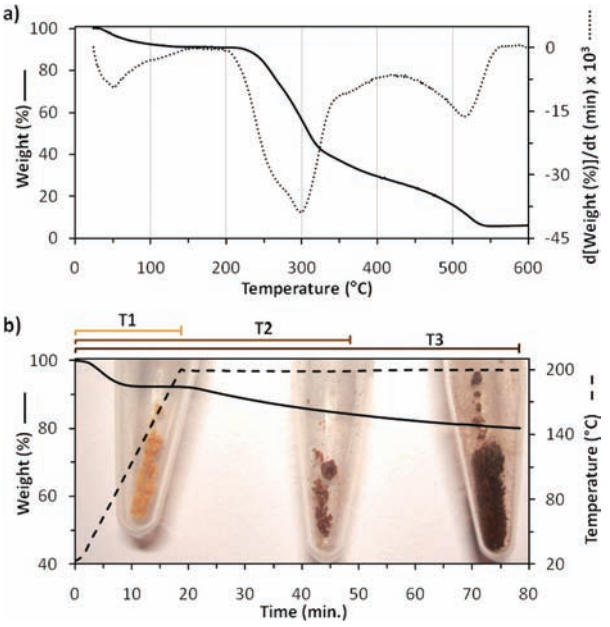


**Figure 1.** (a) TG and DTG curves of β-(1→4)-D-mannotriose ($Man_3$) obtained from room temperature to 600 °C and (b) TG curve of $Man_3$ with illustration of the different thermal treatments (T1, T2, and T3) and the corresponding roasted materials.

**Methylation Analysis.** Both the untreated and thermally treated oligosaccharides were converted to partially O-methylated alditol acetates (PMAA) via successive methylation, hydrolysis, reduction, and acetylation reactions according to the method described by Nunes and Coimbra.[4] The PMAA were dissolved in anhydrous acetone and identified by gas chromatography−mass spectrometry (GC-MS) on an Agilent Technologies 6890N Network (Santa Clara, CA). The GC was equipped with a 400-1HT (Quadrex Corp., Woodbridge, CT) capillary column (25 m length, 0.23 mm internal diameter, and 0.05 μm film thickness). The samples were injected in splitless mode (time of splitless = 6 min), with the injector operating at 220 °C, and using the following temperature program: initial temperature, 50 °C, raised at a rate of 8 °C/min until 140 °C, standing for 5 min at this temperature, followed by a rate of 0.5 °C/min to 150 °C, and then followed by a rate of 40 °C/min to 300 °C, with a further 1 min at 300 °C. The helium carrier gas had a flow rate of 0.2 mL/min and a column head pressure of 12.95 psi. The GC was connected to an Agilent 5973 mass quadrupole selective detector operating with an electron impact mode at 70 eV and scanning the range $m/z$ 40−500 in a 1 s cycle in full-scan mode acquisition.

## RESULTS AND DISCUSSION

**Thermal Stability of the Oligosaccharides.** Thermogravimetric analysis (TG and DTG curves, Figure 1a) of $Man_3$ was carried out from room temperature to 600 °C to determine the thermal stability of this oligosaccharide. In the DTG curve it is possible to observe three main mass loss stages. The first mass

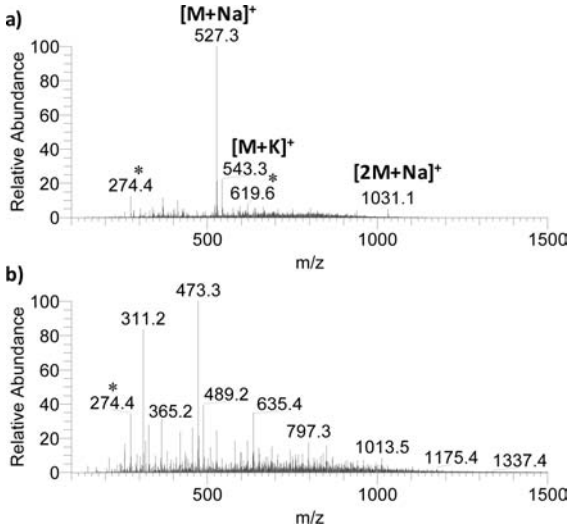


**Figure 2.** ESI-MS spectra obtained for $Man_3$ (a) untreated (T0) and (b) after thermal treatment at 200 °C for 30 min (T2). Ions marked with an asterisk are attributed to impurities.

loss (8.8%) occurring from room temperature to 150 °C should be associated with the evaporation of water molecules adsorbed to the oligosaccharide, as reported in other TG studies.[18,19] The two other main mass loss stages, observed for temperatures higher than 200 °C, are indications of the occurrence of thermal reactions that are accompanied by mass changes. Taking into account that the coffee roasting process is usually performed at temperatures around 200 °C[1] and that at this temperature $Man_3$ seems to be thermally stable, the temperature programs used for thermal treatment of the oligosaccharides under study took into account this maximum.

As illustrated in Figure 1b, $Man_3$ was heated from room temperature to 200 °C, being maintained at 200 °C for different periods of time. When the $Man_3$ was heated to 200 °C (T1), the loss of material was 7.7%, which is in accordance with the amount of water loss observed in Figure 1a, although a light brown colored material was recorded. When the $Man_3$ was maintained at 200 °C during 30 min (T2), the loss of an extra 8.1% of material was observed. On the basis of the brown color of the sample, it can be inferred that this mass loss may be due to the occurrence of thermal reactions that are accompanied by mass changes. The same could be inferred when the material was heated during 60 min at 200 °C (T3) as the loss of an extra 4.2% of material was observed and the material was darker than the previous one. The appearance of the brown coloration is consistent with the formation of brown-colored compounds observed in heated sugar-rich foods as a result of caramelization reactions[20] that were shown to occur during the roasting process of coffee beans.[13] This observation allows the conclusion that caramelization reactions contribute effectively to the brown color development in roasted coffee beans.

The thermal treatments performed for $Man_3$ were also carried out for the other tri- and tetraoligosaccharides related structurally with coffee galactomannans, namely, $GalMan_2$, $Man_4$, and $GalMan_3$. All of these samples acquired the brown coloration reported for $Man_3$ during the thermal treatment. For all oligosaccharides under study, the total mass loss percentages determined from TG curves were 4−10% for T1, 12−16% for T2, and 16−20% for T3. To further characterize the structural changes associated with these thermal treatments, the materials resulting from T1, T2, and T3 of all oligosaccharides under study were analyzed by MS using ESI and MALDI ionization techniques.

**ESI-MS Analysis of Thermally Treated Oligosaccharides.** The ESI-MS spectrum of thermally untreated $Man_3$ (Figure 2a) allowed the observation of the ions at $m/z$ 527 and 543, attributed to the sodium ($[Hex_3 + Na]^+$) and potassium ($[Hex_3 + K]^+$) adduct ions, respectively. Furthermore, an adduct ion formed by two oligosaccharides and one sodium ion ($[2Hex_3 + Na]^+$) at $m/z$ 1031 was also observed. The same $m/z$ ions were observed for $GalMan_2$ (data not shown). The ESI-MS spectra of untreated $Man_4$ and $GalMan_3$ (data not shown) allowed the observation of the ions at $m/z$ 689 and 705, attributed to $[Hex_4 + Na]^+$ and $[Hex_4 + K]^+$, respectively. All oligosaccharides under study ionized predominately as sodium adducts, in accordance with the previous studies on mannosyl oligosaccharides.[9,10,13]

Figure 2b shows the ESI-MS spectrum acquired for $Man_3$ after thermal treatment at 200 °C during 30 min (T2). All $[M + Na]^+$ ions identified in this spectrum and their relative abundances are displayed in Figure 3a. The ions observed at $m/z$ 203, 365, 527, 689, 851, 1013, 1175, and 1337 can be attributed to the sodium adducts of a series from a single hexose to eight hexose residues ($[Hex_{1-8} + Na]^+$). Also, in this spectrum were observed the ions at $m/z$ 347, 509, 671, 833, 995, and 1157, attributed to the sodium adducts of hexose oligosaccharides presenting a loss of one water molecule ($[Hex_{2-7} - H_2O + Na]^+$), as well as the ions at $m/z$ 311, 473, 635, 797, 959, and 1121, attributed to the sodium adducts of hexose oligosaccharides presenting a loss of three water molecules ($[Hex_{2-7} - 3H_2O + Na]^+$). The corresponding potassium adducts of some of these ions were also observed, as, for example, the ion at $m/z$ 489 ($[Hex_3 - 3H_2O + K]^+$). In Figure 3a it is also possible to observe that, with the exception of the ion at $m/z$ 1337 ($[Hex_8 + Na]^+$), the same ions were observed for T2 and T3. For these two treatments, the most intense ions were observed at $m/z$ 311 and 473, attributed to $[Hex_{2-3} - 3H_2O + Na]^+$. For the lightest treatment (T1), the only ion identified beyond the ion at $m/z$ 527 was the ion at $m/z$ 365, attributed to $[Hex_2 + Na]^+$.

The relative abundances of $[M + Na]^+$ ions identified in the ESI-MS spectra of $GalMan_2$, $Man_4$, and $GalMan_3$ (thermally treated) are shown in Figure 3b−d. As shown for $Man_3$, few products were formed when these oligosaccharides were heated from room temperature to 200 °C (T1). After this thermal treatment, the predominant ion observed in the mass spectra occurs at $m/z$ 527 for trisaccharides and $m/z$ 689 for tetrasaccharides, attributed to $[Hex_{3-4} + Na]^+$. Also, products having a lower DP in comparison with the starting material were observed for $Man_4$ and $GalMan_3$, inferred by the presence of the ions at $m/z$ 365 and 527, attributed to $[Hex_{2-3} + Na]^+$. Contrary to the observation for $Man_3$, the mass spectrum of $GalMan_2$ did not show the ion corresponding to the product with DP 2 but showed the presence of the ions with a higher DP than that of the starting oligosaccharide, occurring at $m/z$ 689 ($[Hex_4 + Na]^+$) and 1013 ($[Hex_6 + Na]^+$). For longer times of thermal treatment (T2 and T3), it was possible to observe ions corresponding to products with lower and higher DP than those of the untreated oligosaccharides, as well as the respective ions resulting from the loss of one or three water molecules. The predominant ion observed in the mass spectra acquired after these thermal treatments, except for the treatment T2 of $Man_4$, was the ion at $m/z$ 311 or 473, attributed to $[Hex_{2-3} - 3H_2O + Na]^+$. For $Man_4$ treated during

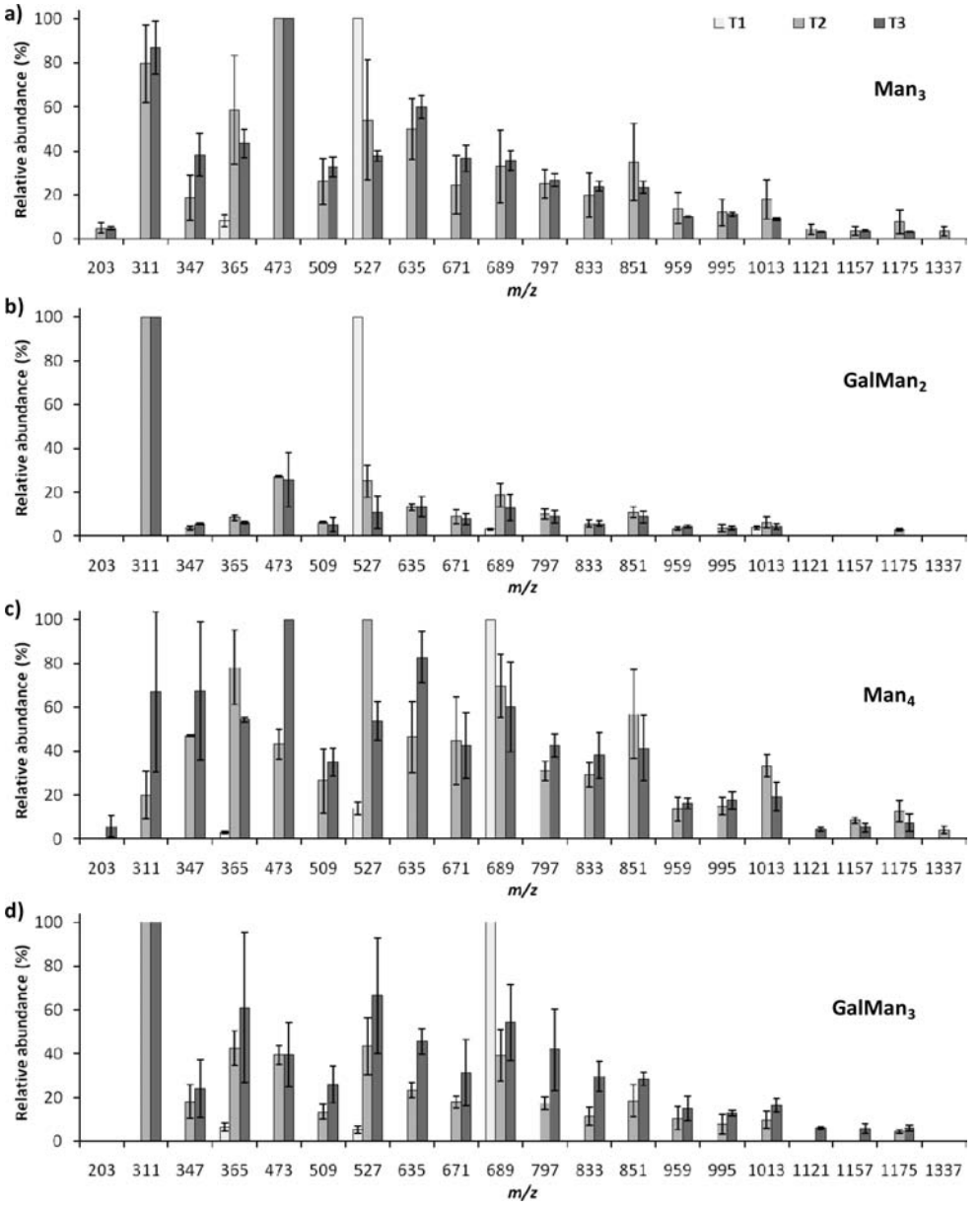


**Figure 3.** Relative abundances of $[M + Na]^+$ ions observed in the ESI-MS spectra of $Man_3$, $GalMan_2$, $Man_4$, and $GalMan_3$ obtained after heating from room temperature to 200 °C and maintaining at 200 °C for 0 min (T1), 30 min (T2), and 60 min (T3). Values are given as the mean ± standard deviation of three replicate spectral acquisitions made on different days. Ions with a mean relative abundance lower than 3% were not considered.

30 min at 200 °C (T2), the predominant ion was observed at $m/z$ 527, attributed to $[Hex_3 + Na]^+$.

The identification of products having a lower DP in comparison with the starting material is in accordance with the decrease of the molecular weight and the degree of branching of roasted coffee extractable galactomannans.[3,4,6,12] The loss of one water molecule was also identified in roasted coffee galactomannans by the detection of 1,6-anhydromannose at the reducing end of these polysaccharides.[13] However, the occurrence of polymerization was never reported to occur in coffee galactomannans with roasting. This may be due to the complexity of the coffee matrix and to the fact that a high fraction of galactomannans remained in the coffee residue after aqueous extraction. This insoluble material, usually associated with the high molecular weight polysaccharides, can have a contribution from the polymerization reactions similar to those observed in this model system. Nevertheless, the formation of oligosaccharides having a higher DP in comparison with the starting oligosaccharide was already reported for dry heating of maltotriose at 200 °C for 30 min.[21] Also, tridehydrated galactomannans from roasted coffee infusions were never identified. However, a revisiting of the pyrolysis−mass spectrometry experiments carried out on amylose and dextran[22] allowed the observation of the possible occurrence of tridehydrated oligosaccharides.

**MALDI-MS Analysis of Thermally Treated Oligosaccharides.** Under ESI-MS conditions, multiple charged ions are commonly observed in the spectra of high molecular weight compounds, making difficult their identification. Because MALDI-MS usually

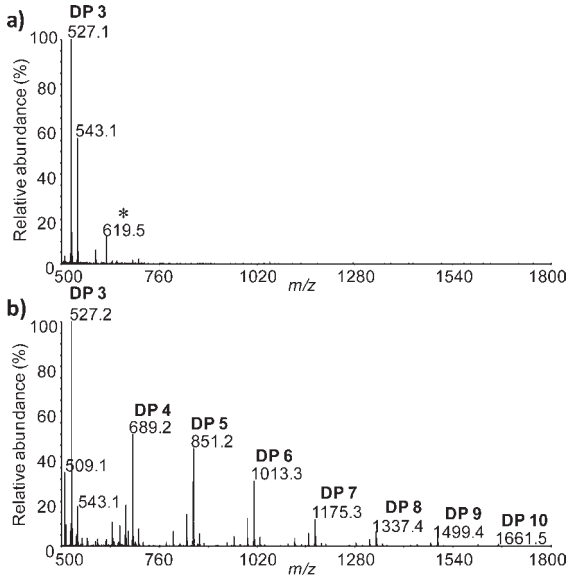


**Figure 4.** MALDI-MS spectra obtained for $Man_3$ (a) untreated (T0) and (b) after thermal treatment at 200 °C for 30 min (T2). The ion marked with an asterisk is attributed to an impurity.

generates only monocharged ions, high molecular weight oligosaccharides are easier to access by MALDI-MS.[17] However, ESI-MS has the advantage of showing low molecular weight compounds, not observable in MALDI-MS spectra due to the interference of matrix ions. To investigate the presence of oligosaccharides with a DP higher than those detected by ESI-MS, a MALDI-MS analysis was performed for all data sets.

By comparison of MALDI-MS spectra obtained for $Man_3$ before (Figure 4a) and after thermal treatment during 30 min at 200 °C (T2) (Figure 4b), it was possible to identify the ions at $m/z$ 527, 689, 851, 1013, 1175, 1337, 1499, and 1661, attributed to $[Hex_{3-10} + Na]^+$, confirming the formation of oligosaccharides with DP higher than that of the starting material. This MS spectrum also showed monodehydrated products present at $m/z$ 509, 671, 833, 995, 1157, 1319, 1481, and 1643 ($[Hex_{3-10} - H_2O + Na]^+$) and tridehydrated products present at $m/z$ 635, 797, 959, 1121, 1283, 1445, and 1607 ($[Hex_{4-10} - 3H_2O + Na]^+$). The ions corresponding to oligosaccharides with 9 and 10 hexose residues were not identified by ESI-MS. The MALDI-MS spectra obtained for all samples (data not shown) allowed confirmation of the previous findings obtained by ESI-MS, which are the polymerization of the oligosaccharides when heated at 200 °C for 30 and 60 min (T2 and T3) and the occurrence of mono- and tridehydrated derivatives of all oligosaccharides formed.

**ESI-MS$^n$ Analysis of Thermally Treated Oligosaccharides.** To confirm the assignments of all sodium adduct ions identified in the ESI-MS spectra as well as to find additional details about their structures, $MS^2$ spectra (and casually $MS^n$ spectra with $n$ to 2) of these ions were acquired. However, only a spectrum for one product of each ion series identified after thermal treatment of $Man_3$ at 200 °C during 30 min (T2) will be explained in detail. $MS^2$ spectra of the same $m/z$ ions obtained for the other thermal treatments as well as the other model oligosaccharides provided the same information.

Previous studies performed on the fragmentation of $[M + Na]^+$ ions of mannosyl oligosaccharides under ESI-$MS^n$ conditions exhibited a characteristic predominant loss of a hexose residue ($Hex_{res}$, −162 Da) due to glycosidic bond cleavage and fragment ions resulting from cross-ring cleavages (cleavage of two bonds within the sugar ring) as well as losses of water (−18 Da).[9,13] The cross-ring cleavages are referred to as neutral losses of $C_2H_4O_2$ (−60 Da), $C_3H_6O_3$ (−90 Da), and $C_4H_8O_4$ (−120 Da), their occurrence being variable with the type of glycosidic linkage.[23,24] Furthermore, studies performed on the fragmentation of $^{18}O$-labeled oligosaccharides composed by hexose residues showed that there is a strong preference for glycosidic bond cleavage on the nonreducing side of the glycosidic oxygen and for cross-ring cleavages on the reducing-end residue.[24,25]

Figure 5a shows the $MS^2$ spectrum of the ion at $m/z$ 527, attributed to $[Hex_3 + Na]^+$, presenting a fragmentation pattern characteristic of $\beta$-(1→4)-linked hexose oligosaccharides.[23,24] It is possible to observe the fragment ions at $m/z$ 365 ($[Hex_2 + Na]^+$) and 203 ($[Hex + Na]^+$) formed by glycosidic bond cleavage with loss of one and two $Hex_{res}$ (−162 Da) from the precursor ion. The fragment ions at $m/z$ 509, resulting from a loss of water (−18 Da) from the precursor ion, and at $m/z$ 467 and 407, resulting from cross-ring cleavages (−60 and −120 Da, respectively) from the precursor ion, are also observed in the spectrum.

Figure 5b shows the $MS^2$ spectrum of the ion at $m/z$ 365, attributed to $[Hex_2 + Na]^+$. In this spectrum, an important point to note is the occurrence of the fragment ion at $m/z$ 275, formed by a mass loss of 90 Da ($C_3H_6O_3$) from the precursor ion, which is not expected to occur for $\beta$-(1→4)-linked oligosaccharides. Because the loss of $C_3H_6O_3$ was reported for (1→3)- and (1→6)-linked oligosaccharides,[23,24] this observation suggests the formation of (1→3) and/or (1→6) glycosidic linkages during the thermal processing of the oligosaccharide under study, resulting from depolymerization and transglycosylation reactions. Transglycosylation reactions are known to occur during the dry thermal processing of oligo- and polysaccharides.[26,27]

Figure 5c shows the $MS^2$ spectrum of the ion at $m/z$ 689, attributed to $[Hex_4 + Na]^+$. This spectrum shows a fragmentation pattern similar to that described for $[Hex_3 + Na]^+$, presenting fragment ions that result from glycosidic cleavages (−162 Da), cross-ring cleavages (−60 and −120 Da), and water losses (−18 Da).

The $MS^2$ spectrum of the ion at $m/z$ 509, attributed to $[Hex_3 - H_2O + Na]^+$ (Figure 5d), shows fragment ions at $m/z$ 347 and 185 formed by loss of one and two $Hex_{res}$ (−162 Da), respectively. The fragment ion at $m/z$ 365, attributed to $[Hex_2 + Na]^+$, formed by loss of an anhydrohexose residue (−144 Da) from the precursor ion, is also observed in the spectrum, indicating that the dehydration may occur in a terminal residue. By comparison of this fragmentation pattern with the nonmodified correspondent oligosaccharide ($[Hex_3 + Na]^+$, Figure 5a), the predominance of the ion at $m/z$ 347 suggests that the anhydrohexose is preferentially positioned at the reducing end of the oligosaccharide. A similar $MS^2$ spectrum was obtained by Nunes et al.[13] after enzymatic hydrolysis of galactomannans from roasted coffee infusions, the precursor ion being assigned as an oligosaccharide with a reducing-end sugar unit modified in the form of 1,6-$\beta$-anhydromannose. Furthermore, 1,6-$\beta$-anhydro-oligosaccharides have also been identified when oligo- and polysaccharides, namely, maltooligosaccharides with DP 2−5[26] and cellulose,[28−30] were submitted to dry heating conditions. However, dehydration occurring from other positions of the reducing-end hexose cannot be excluded.

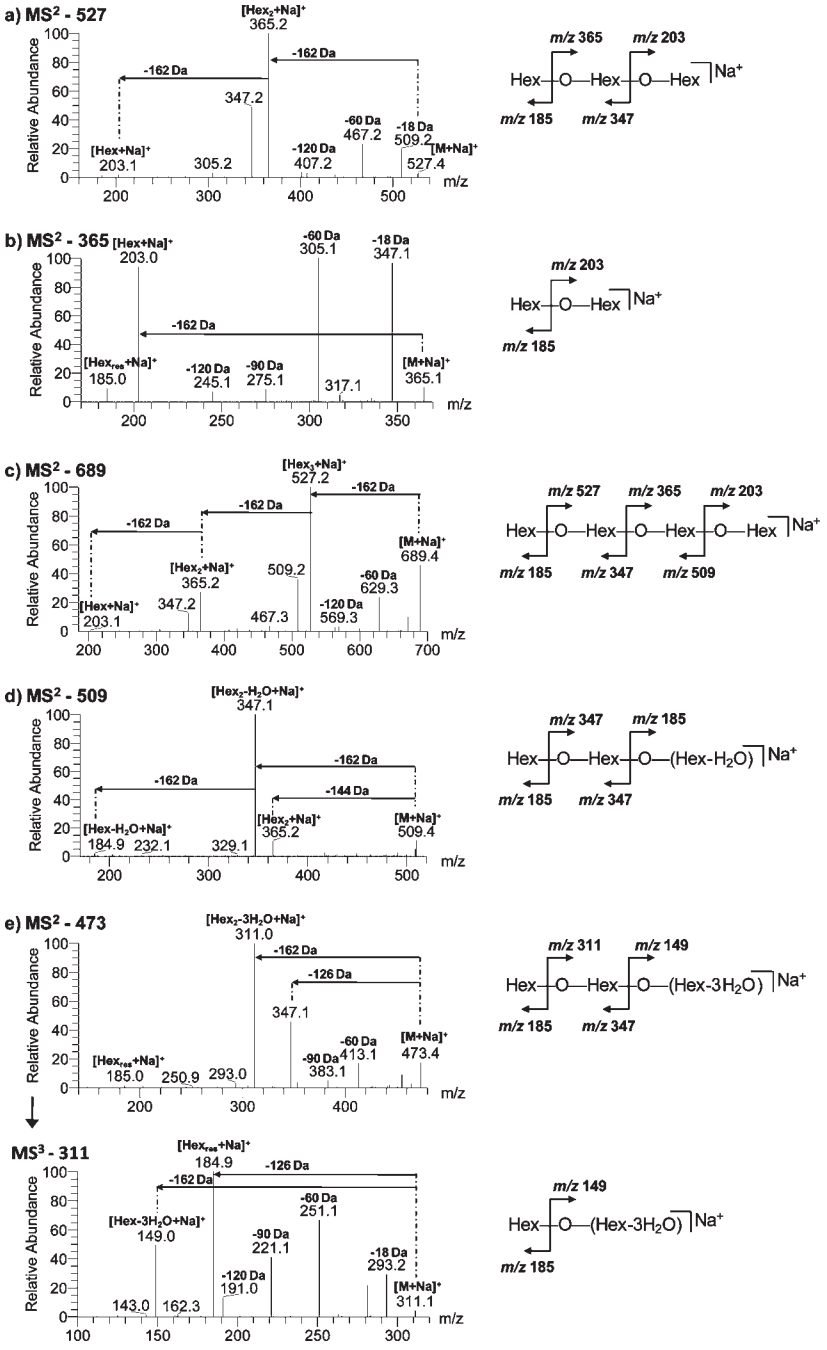


**Figure 5.** ESI-MS$^n$ spectra and schematic fragmentation pathways of $[M + Na]^+$ ions identified after thermal treatment at 200 °C for 30 min (T2) of $Man_3$: (a) $[Hex_3 + Na]^+$; (b) $[Hex_2 + Na]^+$; (c) $[Hex_4 + Na]^+$; (d) $[Hex_3 - H_2O + Na]^+$; (e) $[Hex_3 - 3H_2O + Na]^+$.

Figure 5e shows the MS$^2$ spectrum of the ion at $m/z$ 473, attributed to $[Hex_3 - 3H_2O + Na]^+$. The glycosidic bond cleavage from the nonreducing end was the predominant fragmentation pathway, with the loss of the $Hex_{res}$ (−162 Da) to give a predominant fragment ion at $m/z$ 311, attributed to $[Hex_2 - 3H_2O + Na]^+$. This is an indication that the sugar unit at the nonreducing end is a nonmodified hexose residue. The fragment ion at $m/z$ 347, formed by loss of a trianhydrohexose (−126 Da) from precursor ion, suggests that the losses of water molecules occur in the hexose residue located at the reducing end of the oligosaccharide. Furthermore, the MS$^3$ fragmentation of the fragment ion at $m/z$ 311 (Figure 5e) gave predominant ions at $m/z$ 149 and 185 resulting from the loss of a $Hex_{res}$ (−162 Da) and a trianhydrohexose (−126 Da), respectively. If the reducing-end sugar unit was not modified, the predominant fragment ion formed by glycosidic cleavage would be the ion at $m/z$ 203, attributed to $[Hex + Na]^+$. The fragmentation pattern observed in this MS$^3$ spectrum supports that the loss of three water molecules was occurring at the reducing-end sugar unit of the oligosaccharide.

**Deuterium-Labeling and Alditol Derivatization Experiments.** Although MS$^n$ experiments suggest that the loss of three water molecules in the $[Hex_{2-7} - 3H_2O + Na]^+$ ions occurs at the reducing-end sugar unit of the oligosaccharides,


dx.doi.org/10.1021/jf2021072 |J. Agric. Food Chem. 2011, 59, 10078–10087

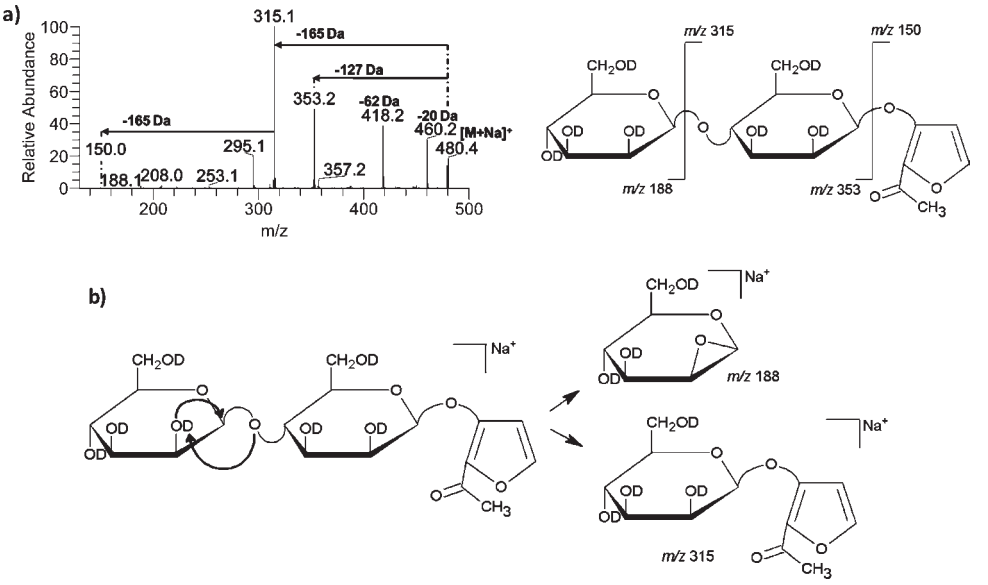


**Figure 6.** (a) ESI-MS$^2$ spectra and schematic fragmentation pathways of the deuterium-labeled ion at $m/z$ 480 corresponding to the ion at $m/z$ 473 in unlabeled sample and (b) mechanism of glycosidic bond cleavage according to Hofmeister et al.[25].

additional experiments were undertaken to unambiguously demonstrate this evidence, namely, deuterium-labeling and alditol derivatization experiments.

A portion of the dissolved material resulting from the thermal treatment of $Man_3$ and $GalMan_2$ during 30 min at 200 °C (T2) was dried and then dissolved in deuterated water for replacement of the hydrogen atoms of hydroxyl groups by deuterium. The ESI-MS$^2$ spectrum of the deuterium-labeled ion at $m/z$ 480, corresponding to the ion at $m/z$ 473 ($[Hex_3 - 3H_2O + Na]^+$, Figure 5e) in the unlabeled $Man_3$ sample, is shown in Figure 6a. The difference between the $m/z$ values of 480 ($[M - 7H + 7D + Na]^+$) and 473 ($[M + Na]^+$) indicates that this tridehydrated product has seven hydroxyl groups in its structure. The main fragment ion occurs at $m/z$ 315, formed by the loss of 165 Da from the precursor ion, by glycosidic bond cleavage according to the mechanism proposed by Hofmeister et al.[25] This mechanism involves the transference of a deuterium atom from an oxygen linked to a carbon from the sugar ring to the glycosidic oxygen as shown in Figure 6b for the formation of the fragment ions occurring at $m/z$ 315 and 188. The two consecutive losses of 165 Da from the precursor ion allow the conclusion that this tridehydrated product has no hydroxyl groups other than those present in the two nonmodified hexose residues. Furthermore, the fragmentation pattern obtained, similar to that observed for the ion at $m/z$ 473 in the unlabeled sample, allows the confirmation of the loss of three water molecules at the reducing-end residue. For $GalMan_2$, the ESI-MS$^2$ spectrum of the deuterium-labeled ion at $m/z$ 315, corresponding to the ion at $m/z$ 311 ($[Hex_2 - 3H_2O + Na]^+$) in the unlabeled sample (data not shown), allowed the same conclusions to be reached. Some studies showed that glucosylisomaltol is formed by heat treatment of foods rich in sugars.[31] Because no hydroxyl groups are present in the reducing-end sugar unit of the tridehydrated oligosaccharides identified in this work, it can be suggested that these tridehydrated products have an isomaltol moiety at the reducing end, as illustrated in Figure 6. Nevertheless, for branched oligosaccharides ($GalMan_2$ and $GalMan_3$), this structure cannot

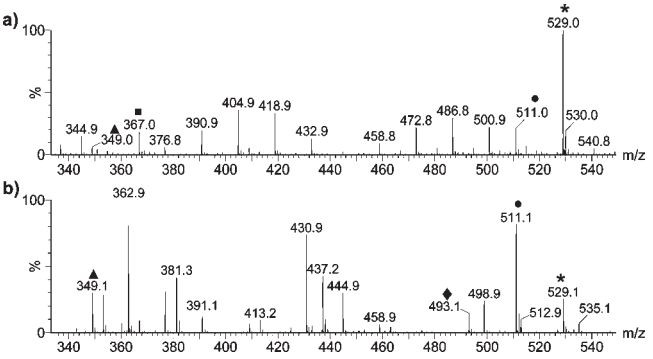


**Figure 7.** ESI-MS spectra of $Man_3$ after reduction and thermal treatment at 200 °C for (a) 0 min (T1) and (b) 30 min (T2): ∗, $[M + Na]^+$ adduct of $Hex_3$ alditol; ●, $[M + Na]^+$ adduct of $Hex_3 - H_2O$ alditol; ◆, $[M + Na]^+$ adduct of $Hex_3 - 2H_2O$ alditol; ■, $[M + Na]^+$ adduct of $Hex_2$ alditol; ▲, $[M + Na]^+$ adduct of $Hex_2 - H_2O$ alditol. Ions not marked by a symbol are due to contaminants arising from the alditol synthesis procedure.

occur without the loss of a galactose residue prior to the formation of the trianhydrous derivative. Alternatively, a different structure may be formed at the reducing mannose residue in branched oligosaccharides.

To evaluate the relevance of the anomeric carbon for the formation of the modifications at the reducing-end residue, $Man_3$ oligosaccharides were converted into their alditol derivatives upon reduction with sodium borohydride and were thermally treated from room temperature to 200 °C (T1) and left at 200 °C during 30 min (T2). For T1, the ESI-MS spectrum (Figure 7a) shows the ions at $m/z$ 529 and 367, corresponding to $[M + Na]^+$ adducts of $Hex_3$ and $Hex_2$ alditols ($Hex_2$Hexol and HexHexol, respectively). The presence of the ion at $m/z$ 367 ($[HexHexol + Na]^+$) and the absence of the ion at $m/z$ 365 ($[Hex_2 + Na]^+$) indicate that the formation of a product with a DP lower than that of the starting material occurs by loss of the non-reducing-end hexose residue. On the other hand, the presence of the ions at

$m/z$ 511 and 349, attributed to $[Hex_{2-1}Hexol - H_2O + Na]^+$, indicates that the alditol derivatization allows the formation of anhydrous products not observed in the ESI-MS spectrum of nonreduced sample subjected to the same thermal treatment (T1). $MS^2$ spectra of these ions (data not shown) showed that the loss of the water molecule occurs exclusively at the hexitol residue. The ESI-MS spectrum obtained for treatment T2 (Figure 7b) shows an ion at $m/z$ 493, attributed to $[Hex_2Hexol - 2H_2O + Na]^+$, a didehydrated derivative not observed in the ESI-MS spectrum of nonreduced sample (Figure 2b). The $MS^2$ spectrum of this ion (data not shown) suggests the presence of two structural isomers, one formed by the loss of two water molecules at the hexitol residue and the other formed by the loss of one water molecule at both sides, the terminal nonreducing residue and at the hexitol residue. Furthermore, an important point to note is the absence of the tridehydrated products, confirming the loss of three water molecules at the reducing-end sugar unit of the oligosaccharides. The MALDI-MS spectrum of the alditol derivative of $Man_3$ treated at 200 °C during 30 min (T2) (data not shown) allowed the observation of the ions at $m/z$ 511 and 529, attributed to $[Hex_2Hexol - H_2O + Na]^+$ and $[Hex_2Hexol + Na]^+$, as already observed by ESI-MS.

These analyses confirm that under the conditions used, neither tridehydrated products nor polymerization products are formed during the thermal processing of the $Man_3$ alditols, highlighting the relevance of the presence of an anomeric carbon for the formation of these products. In fact, as the polymerization observed occurred via transglycosylation, the absence of the anomeric carbon prevents its occurrence. Nevertheless, the depolymerization of these alditol structures would result in the formation of new anomeric carbons able to undergo polymerization. However, this was not observed, suggesting that the extent of the depolymerization reactions is not enough to promote the occurrence of highly abundant polymerized oligosaccharides observed in thermally treated nonreduced samples. Although the polymerization reactions were shown to be more frequent than depolymerization in these oligosaccharides, their extent should be lower for polysaccharides because of the lower proportion of reducing ends in relation to the number of glycosidic linkages that can be cleaved by thermal processing. This is an aspect that deserves research.

**Methylation Analysis.** To compare the type of linkages present in $Man_3$ and $GalMan_2$ before and after thermal treatments of these oligosaccharides, a methylation analysis was performed (Table 1).

For thermally untreated $Man_3$ (T0), T-Man*p* (41.8%) and (1→4)-Man*p* (54.8%) were the most abundant residues. As (1→4)-Man*p* can arise from the reducing end as well as from the middle-chain residue, no quantitative analysis was achieved. A small amount of (1→4)-linked mannose in the open-chain form (4-$Man_{red}$), 2.2%, was also identified. The presence of terminally linked Gal*p* (2.0%) and Glc*p* (0.1%), (1→4)-Glc*p* (0.7%), and (1→4,6)-Man*p* (0.6%) shows that, although in small amounts, oligosaccharides other than $\beta$-(1→4)-D-mannotriose are also present in this sample. The percentage of T-Man*p* from thermally treated samples was higher for longer times of thermal treatment (40.7% for T1, 43.5% for T2, and 51.5% for T3). The percentage of (1→4)-Man*p* decreased from untreated sample to thermally treated samples and from the shorter treatment time to the longest treatment (51.7, 29.4, and 22.4%, respectively). A decrease of T-Gal*p* residues was also observed, varying from 1.9% for T1 to 0.9% for T3. The amount of (1→4,6)-Man*p* increased from the untreated sample to the thermally treated ones (1.5−7.8%). In all thermal treatments, methylation analysis revealed the presence of (1→2)- and (1→6)-Man*p* residues, varying in the ranges of 0.1−2.6 and 1.2−15.7%, respectively. These results show that new types of glycosidic linkages are formed during the thermal treatment. The identification of (1→6)-linked Man*p* residues is in agreement with the cross-ring cleavage fragment ions formed by loss of $C_3H_6O_3$ (−90 Da) observed in the $MS^n$ experiments previously described. An increase of (1→4)-linked Glc*p* residues was also observed from untreated sample to thermally treated samples (2.2−3.4%), showing that isomerization reactions occur during thermal processing, promoting the conversion of mannose into glucose. In chair conformation, $\beta$-D-glucose has all of its substituents in equatorial positions and is thus the most stable hexopyranose.[32] This fact can explain the specific formation of Glc*p* residues during the thermal processing of this model oligosaccharide.

**Table 1. Glycosidic Linkage Composition (Percent Area) of $Man_3$ and $GalMan_2$ before (T0) and after Thermal Processing (T1, T2, and T3)**

| | $Man_3$ | | | | $GalMan_2$ | | | |
|---|---|---|---|---|---|---|---|---|
| linkage | T0 | T1 | T2 | T3 | T0 | T1 | T2 | T3 |
| 4-$Man_{red}$[a] | 2.2 | 0.5 | | | | | | |
| T-Man*p* | 41.8 | 40.7 | 43.5 | 51.5 | 36.8 | 40.8 | 32.5 | 29.0 |
| 2-Man*p* | | 0.1 | 2.6 | 2.0 | | 0.2 | 2.3 | 2.4 |
| 4-Man*p* | 54.8 | 51.7 | 29.4 | 22.4 | 1.6 | 1.3 | 5.2 | 4.6 |
| 6-Man*p* | | 1.2 | 11.5 | 15.7 | 0.4 | 0.6 | 8.4 | 10.7 |
| 4,6-Man*p* | 0.6 | 1.5 | 7.8 | 5.2 | 26.5 | 23.7 | 7.7 | 6.1 |
| T-Gal*p* | 2.0 | 1.9 | 1.5 | 0.9 | 33.5 | 31.5 | 24.6 | 21.7 |
| 2-Gal*p* | | | | | 0.3 | 0.2 | 3.7 | 3.4 |
| 6-Gal*p* | | | | | | | 5.9 | 7.1 |
| T-Glc*p* | 0.1 | 0.2 | 0.4 | | 0.8 | 1.1 | 3.6 | 3.5 |
| 4-Glc*p* | 0.7 | 2.6 | 3.4 | 2.2 | 0.2 | 0.6 | 6.0 | 11.6 |

[a] Reducing terminal residue detected as 1,4-di-*O*-acetyl-1-deuterio-2,3,5,6-tetra-*O*-methylmannitol.

For thermally untreated $GalMan_2$ (T0), T-Man*p* (36.8%) and (1→4,6)-Man*p* (26.5%) as well as T-Gal*p* (33.5%) were the most abundant residues. Small amounts of (1→4)- and (1→6)-Man*p* (1.6 and 0.4%, respectively) as well as (1→2)-Gal*p* (0.3%) and T- and (1→4)-Glc*p* (0.8 and 0.2%, respectively) were also identified, showing that this sample is not composed exclusively by α-(1→6)-D-galactosyl-$\beta$-(1→4)-D-mannobiose. The percentage of T-Man*p* from thermally treated samples, contrary to that observed for $Man_3$, was lower for longer times of thermal treatment (32.5% for T2 and 29.0% for T3), whereas for the lightest treatment (T1) the percentage of T-Man*p* (40.8%) increased in relation to thermally untreated sample. The percentage of (1→4)-Man*p* residues identified for T1 (1.3%) was approximately the same as that observed for T0. However, an increase of (1→4)-Man*p* was observed for longer thermal treatments (5.2% for T2 and 4.6% for T3). A similar behavior was observed for (1→2)-Gal*p*, varying in the range of 0.2−3.7% for thermally treated samples. Also, the percentage of (1→4,6)-Man*p* as well as T-Gal*p* decreased from untreated sample to the thermally treated ones. As observed for $Man_3$, (1→2)- and (1→6)-Man*p* were formed as a consequence of thermal processing, varying in the ranges of 0.2−2.4 and 0.6−10.7%, respectively. For longer thermal treatments (T2 and T3), methylation

analysis also revealed the presence of (1→6)-Gal*p* residues. An increase of T- and (1→4)-Glc*p* was observed from untreated sample to thermally treated samples, varying in the ranges of 1.1−3.6 and 0.6−11.6%, respectively.

The formation of (1→2)- and (1→6)-Man*p* during thermal processing occurs in both oligosaccharides, confirming the occurrence of transglycosylation reactions. The formation of (1→6) glycosidic linkages was previously observed for starch heat treated at low moisture content.[27] Also, an increase of (1→4)-Glc*p* was observed for thermally treated $Man_3$ and $GalMan_2$. In a previous work, it was shown that the galactomannans of the roasted coffee infusions contained (1→4)-Glc residues at the reducing end, contrary to what was observed for green coffee infusions.[9,13] The results obtained in this work suggest that these Glc residues at the reducing end can be formed by an isomerization reaction. The isomerization reaction was already described to occur during the roasting of the coffee by detection of fructose at the reducing end of the galactomannans of coffee infusions.[13] Furthermore, the isomerization process has been observed in various model oligosaccharides heated under dry conditions.[26,33]

In summary, dry thermal treatment of manno-oligosaccharides promotes the occurrence of polymerization, depolymerization, dehydration, and isomerization reactions. New glycosidic linkages are formed via transglycosylation reactions. These reactions can, however, be prevented when the anomeric carbon of the oligosaccharides is reduced or modified. Although these experiments were performed in oligosaccharides, it is expected that similar reactions occur during the roasting of coffee beans, allowing an explanation of the multitude of compounds that are recovered from this matrix.

## AUTHOR INFORMATION

### Corresponding Author

*Phone: +351 234 370706. Fax: +351 234 370084. E-mail: mac@ua.pt.

### Funding Sources

We appreciate the financial support provided to project PTDC/QUI-QUI/100044/2008, QOPNA (Project PEst-C/QUI/UI0062/2011), and RNEM by the Foundation for Science and Technology (FCT).

## ABBREVIATIONS USED

DP, degree of polymerization; $Man_3$, β-(1→4)-D-mannotriose; $GalMan_2$, [α-(1→6)-D-galactosyl]$^1$-β-(1→4)-D-mannobiose; $Man_4$, β-(1→4)-D-mannotetraose; $GalMan_3$, [α-(1→6)-D-galactosyl]$^1$-β-(1→4)-D-mannotriose ($GalMan_3$); $MS^n$, tandem mass spectrometry; ESI, electrospray ionization; MALDI, matrix-assisted laser desorption/ionization; TG, thermogravimetric (curve); DTG, derivative thermogravimetric (curve); PMAA, partially O-methylated alditol acetates; GC-MS, gas chromatography−mass spectrometry; DHB, 2,5-dihydroxybenzoic acid; T0, thermally untreated sample; T1, thermally treated sample from room temperature to 200 °C; T2, thermally treated sample from room temperature to 200 °C and maintained at 200 °C during 30 min; T3, thermally treated sample from room temperature to 200 °C and maintained at 200 °C during 60 min; $Hex_{res}$, hexose residue; 4-$Man_{red}$, (1→4)-linked mannose in the open-chain form; T-Man*p*, terminally linked mannopyranosyl residues; 2-Man*p*, (1→2)-linked mannopyranosyl residues; 4-Man*p*, (1→4)-linked mannopyranosyl residues; 6-Man*p*, (1→6)-linked mannopyranosyl residues; 4,6-Man*p*, (1→4,6)-linked mannopyranosyl residues; T-Gal*p*, terminally linked galactopyranosyl residues; 2-Gal*p*, (1→2)-linked galactopyranosyl residues; 6-Gal*p*, (1→6)-linked galactopyranosyl residues; T-Glc*p*, terminally linked glucopyranosyl residues; 4-Glcp, (1→4)-linked glucopyranosyl residues.

## REFERENCES

(1) Illy, A.; Viani, R. *Espresso Coffee: The Chemistry of Quality*; Academic Press: London, U.K., 1995.

(2) Aryaa, M.; Rao, L. J. M. An impression of coffee carbohydrates. *Crit. Rev. Food Sci. Nutr.* **2007**, *47*, 51–67.

(3) Oosterveld, A.; Harmsen, J. S.; Voragen, A. G. J.; Schols, H. A. Extraction and characterization of polysaccharides from green and roasted *Coffea arabica* beans. *Carbohydr. Polym.* **2003**, *52*, 285–296.

(4) Nunes, F. M.; Coimbra, M. A. Chemical characterization of the high molecular weight material extracted with hot water from green and roasted Arabica coffee. *J. Agric. Food Chem.* **2001**, *49*, 1773–1782.

(5) Redgwell, R. J.; Trovato, V.; Curti, D.; Fischer, M. Effect of roasting on degradation and structural features of polysaccharides in Arabica coffee beans. *Carbohydr. Res.* **2002**, *337*, 421–431.

(6) Nunes, F. M.; Coimbra, M. A. Chemical characterization of the high-molecular-weight material extracted with hot water from green and roasted Robusta coffees as affected by the degree of roast. *J. Agric. Food Chem.* **2002**, *50*, 7046–7052.

(7) Schenker, S.; Handschin, S.; Frey, B.; Perren, R.; Escher, F. Pore structure of coffee beans affected by roasting conditions. *J. Food Sci.* **2000**, *65*, 452–457.

(8) Bradbury, A. G. W.; Halliday, D. J. Chemical structures of green coffee bean polysaccharides. *J. Agric. Food Chem.* **1990**, *38*, 389–392.

(9) Nunes, F. M.; Domingues, M. R.; Coimbra, M. A. Arabinosyl and glucosyl residues as structural features of acetylated galactomannans from green and roasted coffee infusions. *Carbohydr. Res.* **2005**, *340*, 1689–1698.

(10) Simões, J.; Nunes, F. M.; Domingues, M. R. M.; Coimbra, M. A. Structural features of partially acetylated coffee galactomannans presenting immunostimulatory activity. *Carbohydr. Polym.* **2010**, *79*, 397–402.

(11) Oosterveld, A.; Coenen, G. J.; Vermeulen, N. C. B.; Voragen, A. G. J.; Schols, H. A. Structural features of acetylated galactomannans from green *Coffea arabica* beans. *Carbohydr. Polym.* **2004**, *58*, 427–434.

(12) Nunes, F. M.; Coimbra, M. A. Chemical characterization of galactomannans and arabinogalactans from two Arabica coffee infusions as affected by the degree of roast. *J. Agric. Food Chem.* **2002**, *50*, 1429–1434.

(13) Nunes, F. M.; Reis, A.; Domingues, M. R. M.; Coimbra, M. A. Characterization of galactomannan derivatives in roasted coffee beverages. *J. Agric. Food Chem.* **2006**, *54*, 3428–3439.

(14) Fernández, L. E. M. Introduction to ion trap mass spectrometry: application to the structural characterization of plant oligosaccharides. *Carbohydr. Polym.* **2007**, *68*, 797–807.

(15) Zaia, J. Mass spectrometry of oligosaccharides. *Mass Spectrom. Rev.* **2004**, *23*, 161–227.

(16) Reis, A.; Coimbra, M. A.; Domingues, P.; Ferrer-Correia, A. J.; Domingues, M. R. M. Fragmentation pattern of underivatised xylo-oligosaccharides and their alditol derivatives by electrospray tandem mass spectrometry. *Carbohydr. Polym.* **2004**, *55*, 401–409.

(17) Harvey, D. J. Analysis of carbohydrates and glycoconjugates by matrix-assisted laser desorption/ionization mass spectrometry: an update for 2003−2004. *Mass Spectrom. Rev.* **2009**, *28*, 273–361.

(18) Chen, H.; Zhao, W.; Liu, N. Thermal analysis and decomposition kinetics of Chinese forest peat under nitrogen and air atmospheres. *Energy Fuels* **2011**, *25*, 797–803.

(19) Wong, S.-S.; Kasapis, S.; Tan, Y. M. Bacterial and plant cellulose modification using ultrasound irradiation. *Carbohydr. Polym.* **2009**, *77*, 280–287.

(20) Kroh, L. W. Caramelisation in food and beverages. *Food Chem.* **1994**, *51*, 373–379.

(21) Smaniotto, A.; Bertazzo, A.; Comai, S.; Traldi, P. The role of peptides and proteins in melanoidin formation. *J. Mass Spectrom.* **2009**, *44*, 410–418.

(22) Tas, A. C.; Kerkenaar, A.; LaVos, G. F.; van der Greef, J. Pyrolysis-direct chemical ionization mass spectrometry of some biopolymers in the positive and negative ionization mode. *J. Anal. Appl. Pyrolysis* **1989**, *15*, 55–70.

(23) Simões, J.; Domingues, P.; Reis, A.; Nunes, F. M.; Coimbra, M. A.; Domingues, M. R. M. Identification of anomeric configuration of underivatized reducing glucopyranosyl-glucose disaccharides by tandem mass spectrometry and multivariate analysis. *Anal. Chem.* **2007**, *79*, 5896–5905.

(24) Asam, M. R.; Glish, G. L. Tandem mass spectrometry of alkali cationized polysaccharides in a quadrupole ion trap. *J. Am. Soc. Mass Spectrom.* **1997**, *8*, 987–995.

(25) Hofmeister, G. E.; Zhou, Z.; Leary, J. A. Linkage position determination in lithium-cationized disaccharides: tandem mass spectrometry and semiempirical calculations. *J. Am. Chem. Soc.* **1991**, *113*, 5964–5970.

(26) Kroh, L. W.; Jalyschko, W.; Häseler, J. Non-volatile reaction products by heat-induced degradation of α-glucans. Part I: Analysis of oligomeric maltodextrins and anhydrosugars. *Starch/Staerke* **1996**, *48*, 426–433.

(27) Siljeström, M.; Björck, I.; Westerlund, E. Transglycosidation reactions following heat treatment of starch — effects on enzymic digestibility. *Starch/Staerke* **1989**, *41*, 95–100.

(28) Helleur, R. J.; Jackman, P. Thermal fragmentation analysis of neutral polysaccharides and the presence of 1,6-anhydrooligosaccharides. *Can. J. Chem.* **1990**, *68*, 1038–1043.

(29) Pouwels, A. D.; Eijkel, G. B.; Arisz, P. W.; Boon, J. J. Evidence for oligomers in pyrolysates of microcrystalline cellulose. *J. Anal. Appl. Pyrolysis* **1989**, *15*, 71–84.

(30) Lédé, J.; Blanchard, F.; Boutin, O. Radiant flash pyrolysis of cellulose pellets: products and mechanisms involved in transient and steady state conditions. *Fuel* **2002**, *81*, 1269–1279.

(31) Guerra-Hernández, E.; Ramirez-Jiménez, A.; García-Villanova, B. Glucosylisomaltol, a new indicator of browning reaction in baby cereals and bread. *J. Agric. Food Chem.* **2002**, *50*, 7282–7287.

(32) Stick, R. V.; Williams, S. J. *Carbohydrates: The Essential Molecules of Life*, 2nd ed.; Elsevier: Amsterdam, The Netherlands, 2009.

(33) Simkovic, I.; Surina, I.; Vrican, M. Primary reactions of sucrose thermal degradation. *J. Anal. Appl. Pyrolysis* **2003**, *70*, 493–504.